*Article*

# Finding New Molecular Targets of Two Copper(II)-Hydrazone Complexes on Triple-Negative Breast Cancer Cells Using Mass-Spectrometry-Based Quantitative Proteomics

Lucia M. Balsa [1], María R. Rodriguez [1], Verónica Ferraresi-Curotto [2], Beatriz S. Parajón-Costa [1], Ana C. Gonzalez-Baró [1] and Ignacio E. León [1,3,*]

1 CEQUINOR (UNLP, CCT-CONICET La Plata, Asociado a CIC), Departamento de Química, Facultad de Ciencias Exactas, Universidad Nacional de La Plata, La Plata 1900, Argentina
2 Instituto de Física La Plata, IFLP (UNLP, CCT-CONICET La Plata), Departamento de Física, Facultad de Ciencias Exactas, Universidad Nacional de La Plata, La Plata 1900, Argentina
3 Cátedra de Fisiopatología, Departamento de Ciencias Biológicas, Facultad de Ciencias Exactas, Universidad Nacional de La Plata, La Plata 1900, Argentina
* Correspondence: ileon@biol.unlp.edu.ar

**Abstract:** Breast cancer is the most common cancer in women, with a high incidence estimated to reach 2.3 million by 2030. Triple-Negative Breast Cancer (TNBC) is the greatest invasive class of breast cancer with a poor prognosis, due to the side-effects exerted by the chemotherapy used and the low effectivity of novel treatments. In this sense, copper compounds have shown to be potentially effective as antitumor agents, attracting increasing interest as alternatives to the usually employed platinum-derived drugs. Therefore, the aim of this work is to identify differentially expressed proteins in MDA-MB-231 cells exposed to two copper(II)-hydrazone complexes using label-free quantitative proteomics and functional bioinformatics strategies to identify the molecular mechanisms through which these copper complexes exert their antitumoral effect in TNBC cells. Both copper complexes increased proteins involved in endoplasmic reticulum stress and unfolded protein response, as well as the downregulation of proteins related to DNA replication and repair. One of the most relevant anticancer mechanisms of action found for CuHL1 and CuHL2 was the down-regulation of gain-of-function-mutant p53. Moreover, we found a novel and interesting effect for a copper metallodrug, which was the down-regulation of proteins related to lipid synthesis and metabolism that could lead to a beneficial decrease in lipid levels.

**Keywords:** breast cancer; molecular targets; metallodrugs; copper(II); proteomics

## 1. Introduction

Cancer is one of the main causes of death worldwide [1]. Breast cancer is the most common cancer in women worldwide and one of the more frequent causes of premature mortality in the female population [2]. There are two types of breast cancer, ductal and lobular, which are divided into invasive and in situ (non-invasive) types, with several subtypes based on histology features. One of the most aggressive classes of breast cancer is the Triple-Negative Breast Cancer (TNBC), which does not express estrogen, progesterone, and HER-2 receptors [3]. For TNBC, the treatment options are limited to chemotherapy, including anthracyclines (doxorubicin and epirubicin), taxanes (paclitaxel and docetaxel), and capecitabine, as hormone or targeted therapy cannot be utilized [4]. Platinum chemotherapeutics such as carboplatin are also used [5]. Nevertheless, these treatments present a low efficacy as they produce important adverse effects and a high rate of metastatic recurrence [6]. Therefore, great efforts are dedicated to developing new strategies using therapeutic agents to improve and optimize the treatment. To this end, several metal-based drugs including palladium [7], ruthenium [8,9], and copper [10] were designed and many of them displayed antitumor activity on breast cancer cells.

In this sense, copper compounds offer a promising and innovative alternative to breast cancer treatment. Interest in them arises from the knowledge that copper can play an important role as a limiting factor in different aspects of tumor progression, such as growth, angiogenesis, and metastasis [11]. Several copper compounds showed promising antitumor and anti-metastatic properties on diverse kinds of solid tumors [12–14]. The main mechanisms of action reported involve reactive oxygen species (ROS) generation, glutation (GSH) depletion, proteasome inhibition, and DNA damage [15–19]. However, details of the cell signaling and molecular mechanism of copper complexes are mainly still unanswered.

Proteomics is a very powerful research tool for cellular processes as it provides detailed information of the fine alterations in cell homeostasis triggered by exposure to drugs. Alterations in intracellular signaling and metabolic pathways may tell us which parts of the cellular machinery are mainly affected by treatment, thus suggesting the most probable biomolecular targets for the compound [20].

We have previously reported the synthesis, physicochemical characterization, and anti-tumoral activity of two copper(II)-hydrazone complexes, [Cu(HL1)(H$_2$O)](NO$_3$). H$_2$O and [Cu(HL2)(H$_2$O)$_2$](NO$_3$), or CuHL1 [21,22] and CuHL2 [23] for simplicity. In vitro studies revealed a promising anticancer activity of both complexes against breast cancer cell lines, including the TNBC line MDA-MB-231. Moreover, some possible action mechanisms were demonstrated, such as DNA damage, ROS production, and proteasome inhibition [22,23]. However, the key signal pathways underlying the anticancer mechanism and the therapeutic targets of CuHL1 and CuHL2 have not yet been well characterized. Therefore, this study was initiated to identify differentially expressed proteins in MDA-MB-231 cells exposed to CuHL1 and CuHL2 treatment, using label-free quantitative proteomics and functional bioinformatics strategies to identify the molecular mechanisms through which these copper complexes exert their antitumoral effect in TNBC cells.

## 2. Results and Discussion

### 2.1. Synthesis and Characterization of the Copper Complexes

The compounds CuHL1 and CuHL2 (Figure 1) were obtained following the procedure described in our previous works. They crystallize as complex cations with a +1 charge and with nitrate as a counterion [21,23].
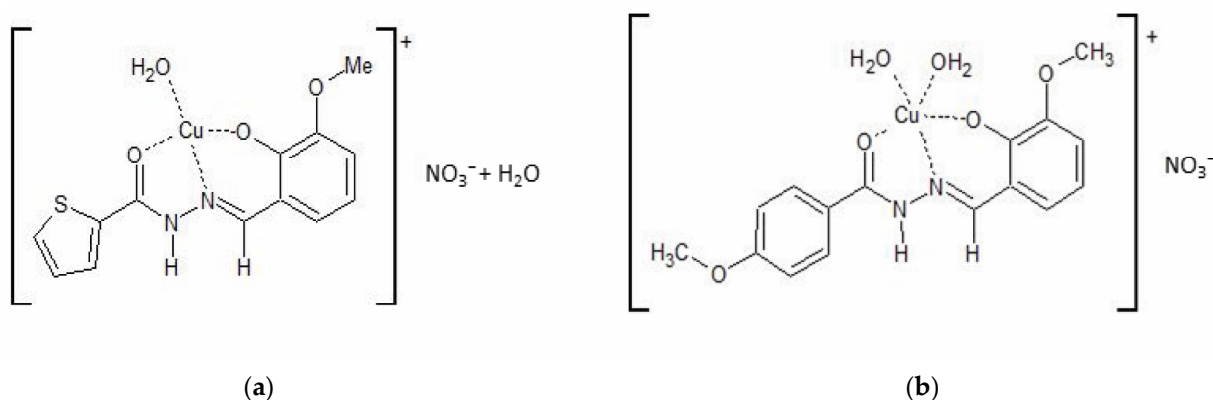


(**a**)                    (**b**)

**Figure 1.** Schematic representation of (**a**) CuHL1 and (**b**) CuHL2.

The corresponding hydrazone (H$_2$L1: 2-acetylthiophene-2-hydroxy-3-methoxybenzohydrazone and H$_2$L2: 2-acetyl-4-methoxyphenyl-2-hydroxy-3-methoxybenzohydrazone) coordinates to the metal as a monoanionic ligand (HL$^-$), by deprotonation of the phenolic oxygen, through the ONO chelating system. The coordination sphere of CuHL1 and CuHL2 is completed with one and two water molecules, respectively, according to the previously reported crystallographic results.

In previous works, we have demonstrated their antitumoral activities against breast cancer cells. Both complexes impaired cell viability in the sub-micromolar concentration

range (0.5–2 μM) against breast cancer cell lines. Particularly, the $IC_{50}$ values in the TNBC cell line MDA-MB-231 are $1.6 \pm 0.2$ μM (CuHL1) and $1.6 \pm 0.1$ μM (CuHL2) [22,23].

### 2.2. Label-Free Mass Spectroscopy Quantification of Proteins Isolated from MDA-MB-231 Cells following Treatment with CuHL1 and CuHL2

To explore the anticancer mechanism of CuHL1 and CuHL2, we conducted label-free quantitative proteomics profiling.

Label-free quantification using the Orbitrap LC–MS/MS (Thermo Scientific™, Waltham, MA, USA) was able to identify proteins that are differentially expressed between cells treated with CuHL1 or CuHL2 and untreated conditions. A total of 1656 and 1659 proteins were identified for CuHL1- and CuHL2-treated cells, respectively. The resulting proteomic dataset was filtered by fold-change differences and a significant *p*-value (Figure 2). From the CuHL1-treated cells, a total of 69 proteins were identified to be differentially expressed when compared with the untreated control (Table 1). Among these differentially expressed proteins, 28 proteins were up-regulated and 41 proteins were down-regulated. As from the CuHL2-treated cells, a total of 63 proteins were identified to be differentially expressed when compared with the basal condition (Table 2). Among these differentially expressed proteins, 23 were up-regulated and 40 were down-regulated by the treatment.
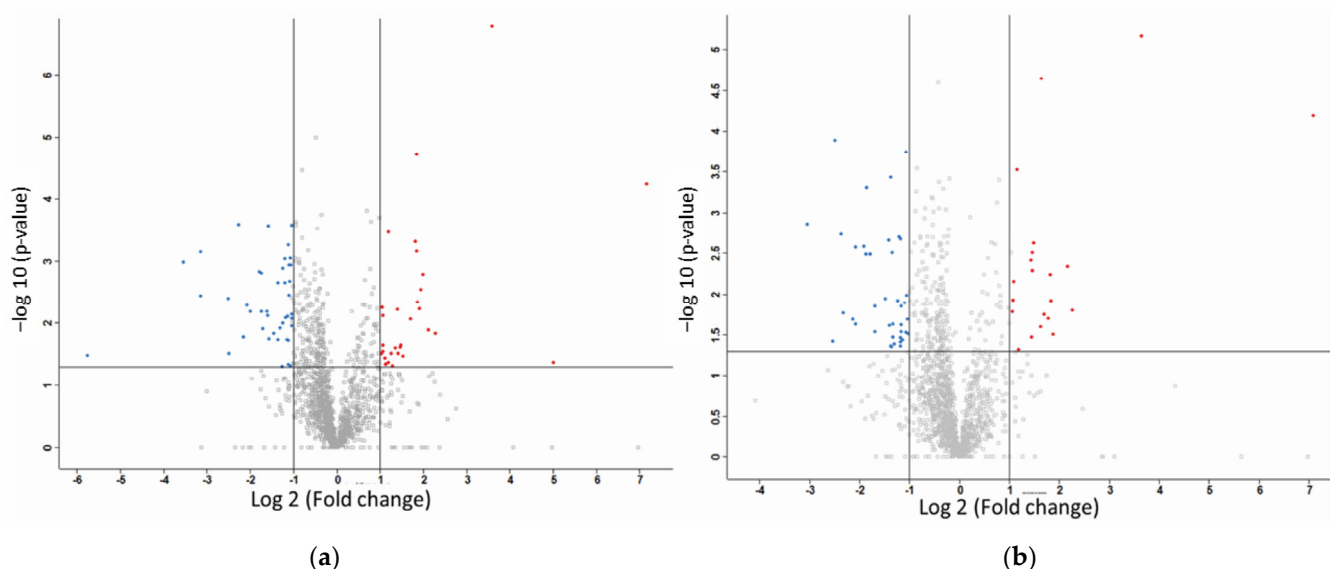


(**a**)                                              (**b**)

**Figure 2.** Volcano plots showing the variation in log10 (*p* value) with log2 (fold change) for various pairwise comparisons: (**a**) CuHL1 vs. Control and (**b**) CuHL2 vs. Control. Color map: grey: not significant, red: up-regulated, blue: down-regulated.

**Table 1.** Differentially expressed proteins in CuHL1-treated MDA-MB.231 cells.

| Gene | Protein | Fold-Change | *p*-Value |
|---|---|---|---|
| HSPA1B | Heat shock 70 kDa protein 1B | 11.9067 | 0.0000 |
| SRXN1 | Sulfiredoxin-1 | 4.8384 | 0.0144 |
| CSTF3 | Cleavage stimulation factor subunit 3 | 4.3157 | 0.0128 |
| THBS1 | Thrombospondin-1 | 3.9412 | 0.0016 |
| CHORDC1 | Cysteine and histidine-rich domain-containing protein 1 | 3.8146 | 0.0028 |
| BAG3 | BAG family molecular chaperone regulator 3 | 3.7564 | 0.0058 |
| SLC25A3 | Phosphate carrier protein, mitochondrial | 3.6397 | 0.0046 |
| HSPH1 | Heat shock protein 105 kDa | 3.5744 | 0.0007 |

**Table 1.** *Cont.*

| Gene | Protein | Fold-Change | *p*-Value |
|------|---------|-------------|-----------|
| DNAJB1 | DnaJ homolog subfamily B member 1 | 3.5735 | 0.0000 |
| GCLM | Glutamate–cysteine ligase regulatory subunit | 3.4930 | 0.0005 |
| SLC25A5 | ADP/ATP translocase 2 | 3.2590 | 0.0085 |
| ARF3 | ADP-ribosylation factor 3 | 2.8776 | 0.0335 |
| MAP1LC3B2 | Microtubule-associated proteins 1A/1B light chain 3 beta 2 | 2.7896 | 0.0222 |
| DDX21 | Nucleolar RNA helicase 2 | 2.7624 | 0.0244 |
| KTN1 | Kinectin | 2.6451 | 0.0302 |
| MMP1 | Interstitial collagenase | 2.6260 | 0.0060 |
| ACTC1 | Actin, alpha cardiac muscle 1 | 2.5367 | 0.0247 |
| FUS | RNA-binding protein FUS | 2.3718 | 0.0305 |
| DNAJA1 | DnaJ homolog subfamily A member 1 | 2.2815 | 0.0003 |
| TECR | Very-long-chain enoyl-CoA reductase | 2.2753 | 0.0422 |
| ARHGEF18 | Rho guanine nucleotide exchange factor 18 | 2.1868 | 0.0453 |
| RPL12 | 60S ribosomal protein L12 | 2.1825 | 0.0442 |
| ZNF622 | Zinc finger protein 622 | 2.1629 | 0.0360 |
| RPL21 | 60S ribosomal protein L21 | 2.0765 | 0.0283 |
| TOP2A | DNA topoisomerase 2-alpha | 2.0762 | 0.0075 |
| RPS8 | 40S ribosomal protein S8 | 2.0729 | 0.0227 |
| RPL7A | 60S ribosomal protein L7a | 2.0663 | 0.0055 |
| RPL10 | 60S ribosomal protein L10 | 2.0453 | 0.0303 |
| SDC4 | Syndecan-4 | −54.1800 | 0.0332 |
| CYP51A1 | Lanosterol 14-alpha demethylase | −11.7752 | 0.0010 |
| FADS2 | Fatty acid-desaturase | −8.9256 | 0.0007 |
| ALG2 | Alpha-1,3/1,6-mannosyltransferase ALG2 | −8.8383 | 0.0036 |
| RRM2 | Ribonucleoside-diphosphate reductase subunit M2 | −5.7327 | 0.0040 |
| SMCHD1 | Structural maintenance of chromosomes flexible hinge domain-containing protein 1 | −5.6365 | 0.0302 |
| DPYD | Dihydropyrimidine dehydrogenase [NADP(+)] | −4.8430 | 0.0003 |
| POLD1 | DNA polymerase | −4.4882 | 0.0165 |
| NFKB2 | Nuclear factor NF-kappa-B p100 subunit | −4.2297 | 0.0051 |
| IRF2BPL | Probable E3 ubiquitin-protein ligase IRF2BPL | −3.9927 | 0.0064 |
| TP53 | Cellular tumor antigen p53 | −3.4861 | 0.0015 |
| LDLR | Low-density lipoprotein receptor (Fragment) | −3.3732 | 0.0065 |
| TMX1 | Thioredoxin-related transmembrane protein 1 | −3.3412 | 0.0015 |
| PSMD4 | 26S proteasome non-ATPase regulatory subunit 4 | −3.3016 | 0.0123 |
| DNAAF5 | Dynein axonemal assembly factor 5 | −3.0889 | 0.0065 |
| TST | Thiosulfate sulfurtransferase | −3.0300 | 0.0075 |
| PXDN | Peroxidasin homolog | −3.0016 | 0.0003 |
| OGFR | Opioid growth factor receptor | −2.9898 | 0.0177 |
| ENG | Endoglin | −2.7407 | 0.0145 |
| FAF1 | FAS-associated factor 1 | −2.5783 | 0.0183 |

**Table 1.** *Cont.*

| Gene | Protein | Fold-Change | *p*-Value |
|------|---------|-------------|-----------|
| MCM5 | DNA replication licensing factor MCM5 | −2.5649 | 0.0022 |
| ADSS2 | Adenylosuccinate synthetase isozyme 2 | −2.4898 | 0.0118 |
| GIPC1 | PDZ domain-containing protein GIPC1 | −2.4031 | 0.0494 |
| ACO1 | Cytoplasmic aconitate hydratase | −2.3932 | 0.0013 |
| PRPSAP2 | Phosphoribosyl pyrophosphate synthase-associated protein 2 | −2.3817 | 0.0099 |
| DNAJA3 | DnaJ homolog subfamily A member 3, mitochondrial | −2.3163 | 0.0022 |
| DLAT | Dihydrolipoyllysine-residue acetyltransferase component of pyruvate dehydrogenase complex, mitochondrial | −2.3145 | 0.0009 |
| SNX5 | Sorting nexin-5 | −2.2927 | 0.0082 |
| PCK2 | Phosphoenolpyruvate carboxykinase [GTP], mitochondrial | −2.2247 | 0.0184 |
| IGFBP7 | Insulin-like growth factor-binding protein 7 | −2.2145 | 0.0077 |
| NDRG3 | N-myc downstream-regulated gene 3 protein | −2.1762 | 0.0005 |
| KRT73 | Keratin, type II cytoskeletal 73 | −2.1747 | 0.0458 |
| PC | Pyruvate carboxylase, mitochondrial | −2.1747 | 0.0187 |
| CORO7 | Coronin | −2.1529 | 0.0035 |
| POLDIP2 | Polymerase delta-interacting protein 2 | −2.1529 | 0.0011 |
| ACOT2 | Acyl-coenzyme A thioesterase 2, mitochondrial | −2.1328 | 0.0021 |
| MAP2K2 | Dual-specificity mitogen-activated protein kinase kinase 2 | −2.1182 | 0.0009 |
| MAGED2 | Melanoma-associated antigen D2 | −2.1069 | 0.0476 |
| IDH3A | Isocitrate dehydrogenase [NAD] subunit alpha, mitochondrial | −2.0820 | 0.0012 |
| ALDH2 | Aldehyde dehydrogenase, mitochondrial | −2.0759 | 0.0003 |
| SLC9A3R1 | Na(+)/H(+) exchange regulatory cofactor NHE-RF1 | −2.0756 | 0.0071 |

**Table 2.** Differentially expressed proteins in CuHL2-treated MDA-MB-231 cells.

| Gene | Protein | Fold-Change | *p*-Value |
|------|---------|-------------|-----------|
| HSPA6 | Heat shock 70 kDa protein 6 | 135.1126 | 0.0001 |
| HSPA1B | Heat shock 70 kDa protein 1B | 12.4443 | 0.0000 |
| SRXN1 | Sulfiredoxin-1 | 4.7883 | 0.0157 |
| BAG3 | BAG family molecular chaperone regulator 3 | 4.4887 | 0.0045 |
| G3BP2 | Ras GTPase-activating protein-binding protein 2 | 3.6714 | 0.0310 |
| THBS1 | Thrombospondin-1 | 3.5660 | 0.0120 |
| CHORDC1 | Cysteine and histidine-rich domain-containing protein 1 | 3.5336 | 0.0057 |
| FXR2 | Fragile X mental retardation syndrome-related protein 2 | 3.4133 | 0.0198 |
| SLC25A3 | Phosphate carrier protein, mitochondrial | 3.2324 | 0.0178 |
| DNAJB1 | DnaJ homolog subfamily B member 1 | 3.0959 | 0.0000 |
| SLC25A5 | ADP/ATP translocase 2 | 3.0855 | 0.0253 |
| GCLM | Glutamate–cysteine ligase regulatory subunit | 2.8046 | 0.0024 |
| ATAD3A | ATPase family AAA domain-containing protein 3A | 2.7501 | 0.0031 |
| MMP1 | Interstitial collagenase | 2.7465 | 0.0051 |
| MAP1LC3B2 | Microtubule-associated proteins 1A/1B light chain 3 beta 2 | 2.7147 | 0.0338 |
| HSPH1 | Heat shock protein 105 kDa | 2.7037 | 0.0038 |
| SDHA | Succinate dehydrogenase [ubiquinone] flavoprotein subunit, mitochondrial | 2.2722 | 0.0472 |
| DNAJA1 | DnaJ homolog subfamily A member 1 | 2.2136 | 0.0003 |
| ZNF622 | Zinc finger protein 622 | 2.1139 | 0.0070 |
| AKAP2 | A-kinase anchor protein 2 | 2.0990 | 0.0117 |
| TMCO1 | Calcium-load-activated calcium channel | 2.0869 | 0.0164 |
| SLC3A2 | 4F2 cell-surface antigen heavy chain | 2.0386 | 0.0031 |
| AHSA1 | Activator of 90 kDa heat shock protein ATPase homolog 1 | 1.9963 | 0.0228 |
| SMCHD1 | Structural maintenance of chromosomes flexible hinge domain-containing protein 1 | −8.2820 | 0.0014 |
| NFKB2 | Nuclear factor NF-kappa-B p100 subunit | −5.8093 | 0.0379 |

**Table 2.** *Cont.*

| Gene | Protein | Fold-Change | *p*-Value |
|---|---|---|---|
| DPYD | Dihydropyrimidine dehydrogenase [NADP(+)] | −5.6316 | 0.0001 |
| RRM2 | Ribonucleoside-diphosphate reductase subunit M2 | −5.2034 | 0.0018 |
| FADS2 | Acyl-CoA 6-desaturase | −5.0562 | 0.0169 |
| DNAAF5 | Dynein axonemal assembly factor 5 | −4.3873 | 0.0202 |
| U2AF1 | Splicing factor U2AF 35 kDa subunit | −4.2363 | 0.0027 |
| SDC4 | Syndecan-4 | −4.2206 | 0.0232 |
| ACSL4 | Long-chain-fatty-acid–CoA ligase 4 | −3.7610 | 0.0026 |
| CYP51A1 | Lanosterol 14-alpha demethylase | −3.6858 | 0.0032 |
| TP53 | Cellular tumor antigen p53 | −3.6284 | 0.0005 |
| GFM1 | Elongation factor G, mitochondrial | −3.4629 | 0.0032 |
| LDLR | Low-density lipoprotein receptor | −3.2341 | 0.0284 |
| OGFR | Opioid growth factor receptor OS = Homo sapiens | −3.2299 | 0.0139 |
| RIN1 | Ras and Rab interactor 1 | −2.7981 | 0.0113 |
| FAF1 | FAS-associated factor 1 | −2.6790 | 0.0022 |
| MCM2 | DNA replication licensing factor MCM2 | −2.6450 | 0.0239 |
| PCK2 | Phosphoenolpyruvate carboxykinase [GTP], mitochondrial | −2.6115 | 0.0004 |
| SUMF2 | Inactive C-alpha-formylglycine-generating enzyme 2 | −2.5908 | 0.0432 |
| HNRNPUL1 | Heterogeneous nuclear ribonucleoprotein U-like protein 1 | −2.5669 | 0.0440 |
| PXDN | Peroxidasin homolog | −2.5552 | 0.0031 |
| MCM3 | DNA replication licensing factor MCM3 | −2.5299 | 0.0332 |
| DNAJA3 | DnaJ homolog subfamily A member 3, mitochondrial | −2.5193 | 0.0231 |
| PACS1 | Phosphofurin acidic cluster sorting protein 1 | −2.4865 | 0.0405 |
| POGLUT3 | Protein O-glucosyltransferase 3 | −2.3599 | 0.0119 |
| SCYL1 | N-terminal kinase-like protein | −2.3123 | 0.0020 |
| FASN | Fatty acid synthase | −2.2785 | 0.0382 |
| VIM | Vimentin | −2.2682 | 0.0343 |
| MCM5 | DNA replication licensing factor MCM5 | −2.2670 | 0.0021 |
| TRIM28 | Transcription intermediary factor 1-beta | −2.2658 | 0.0431 |
| CDC37 | Hsp90 co-chaperone Cdc37 | −2.2547 | 0.0236 |
| YARS2 | Tyrosine–tRNA ligase, mitochondrial | −2.2501 | 0.0139 |
| SMC2 | Structural maintenance of chromosomes protein 2 | −2.2447 | 0.0288 |
| ITGB4 | Integrin beta-4 | −2.2163 | 0.0362 |
| PTK7 | Inactive tyrosine-protein kinase 7 | −2.1469 | 0.0128 |
| CORO7 | Coronin | −2.1154 | 0.0290 |
| ACOT2 | Acyl-coenzyme A thioesterase 2, mitochondrial | −2.1016 | 0.0002 |
| TBC1D9B | TBC1 domain family member 9B | −2.0811 | 0.0103 |
| MYO18A | Unconventional myosin-XVIIIa | −2.0581 | 0.0201 |
| CALM2 | Calmodulin-2 | −2.0396 | 0.0306 |

A comparative analysis of differentially expressed proteins between treatments showed 32 proteins in common. Among down-regulated proteins, the treatments with CuHL1 and CuHL2 shared 18 proteins: TP53, MCM5, PCK2, CORO7, ACOT2, OGFR, FAF1, LDLR, NFKB2, DPYD, DNAAF4, PXDN, RRM2, FADS2, CYP51A1, SMCHD1, SDC4, and DNAJA3. Meanwhile, among up-regulated proteins, the complexes shared 14 proteins: HSPA1B, HSPH1, DNAJB1, DNAJA1, CHORDC1, BAG3, ZNF622, THBS1, MAP1LC3B2, SLC25A3, GCLM, MMP1, SRXN1, and SLC25A5.

### 2.3. Functional GO Enrichment Analysis

To better understand the biological characteristics of the differentially expressed proteins, a set of bioinformatics tools were applied. First, the STRING enrichment analysis was used to study whether any Gene Ontology (GO) categories were statistically enriched. For each complex, two different lists containing the up-regulated and down-regulated proteins were uploaded. The GO database classifies functions in organisms into three categories: the involved biological process, the molecular function, and the cell component. Figure 3 displays the obtained GO terms statistically over-represented (*p*-value $\leq 0.05$ after Benjamini correction). CuHL1 did not show enriched terms of molecular functions for down-regulated proteins, while CuHL2 did not show enriched terms of the cell component for up-regulated proteins.
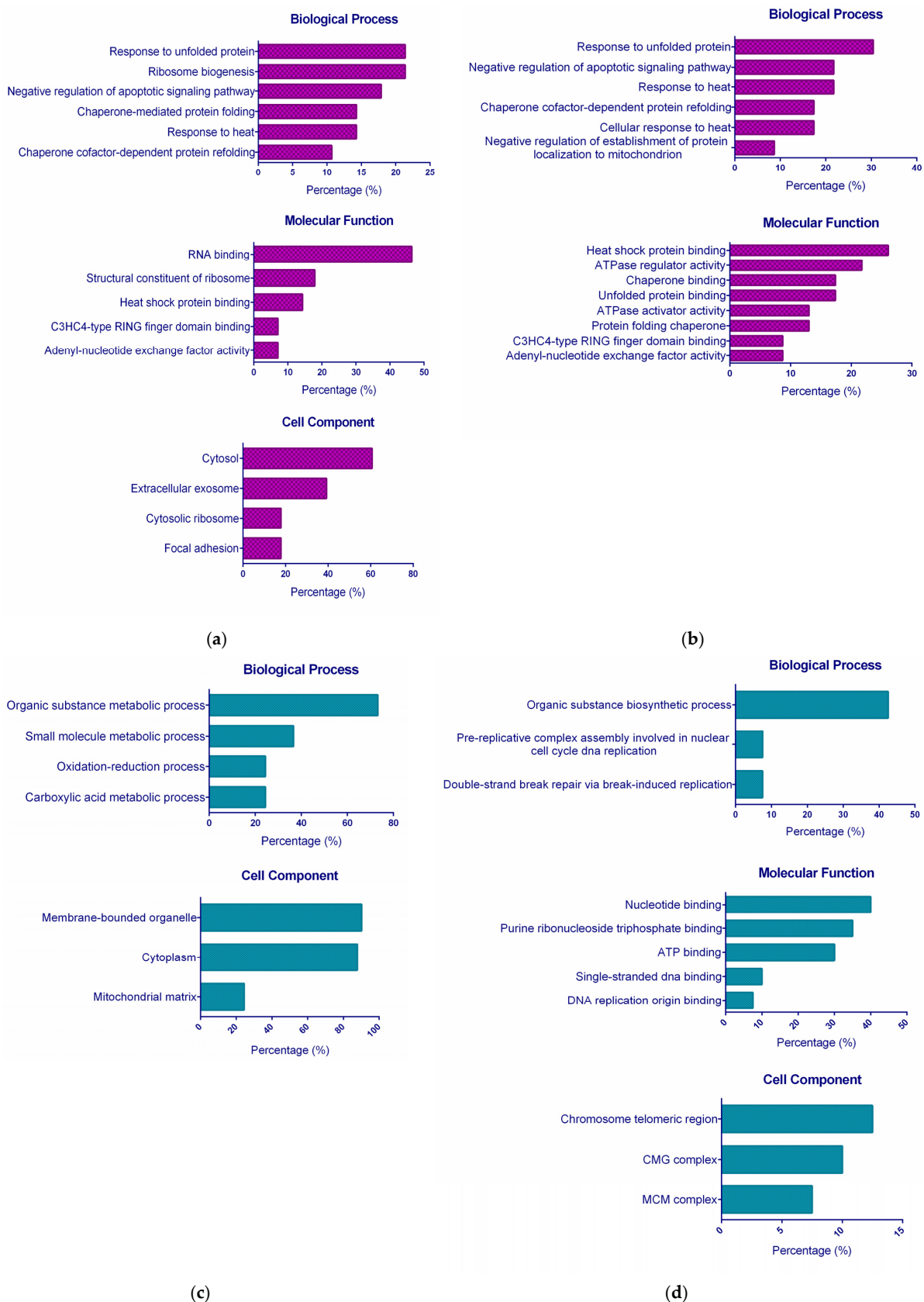
**Figure 3.** GO enrichment analysis of (**a**,**b**) up-regulated proteins after treatment with (**a**) CuHL1 and (**b**) CuHL2; (**c**,**d**) down-regulated proteins after treatment with (**c**) CuHL1 and (**d**) CuHL2. The percentage (%) of representation of each category was determined as a percentage of the total differentially expressed protein.

Among up-regulated proteins, the principal biological processes enriched for both complexes were related to Heat Shock Proteins (HSPs) and co-chaperones: "Response to unfolded protein", "Response to heat", and "Chaperone cofactor-dependent protein refolding". The proteins involved in these processes are HSPs and co-chaperones, mainly from the HSP70 family (HSPA1B, HSPH1, HSPA6, BAG3, DNAJA1, and DNAJB1). In terms of molecular function, mostly proteins assigned to the binding activity associated with HSPs and co-factors could be found for CuHL1 and CuHL2.

An increase in HSP expression levels upon treatment with anticancer agents has been reported. These proteins may participate in the stress response to drug-induced damage [24]. HSPs are involved in protein folding and are generally expressed as a reaction to endoplasmic reticulum stress. Cancer cells have enhanced ER stress due to several characteristics, such as hypoxia, low nutrient availability, lactic acidosis, oxidative stress, and increased replication and metabolism, which leads to increased protein folding and accumulation of misfolded proteins. In response to ER stress, the Unfolded Protein Response (UPR) is initiated [25]. The primary aim of UPR is to re-establish ER homeostasis by increasing the protein-folding capacity [26]. Cancer cells up-regulate the UPR pathway to increase their ability to survive under heightened ER stress. However, if the ER stress is prolonged or acute, a terminal UPR program promotes cell death. In this sense, many cancers with enhanced UPR can be hypersensitive to compounds that generate ER stress. Chemotherapeutics can achieve UPR disruption via different mechanisms such as inhibition of proteasome activity, oxidative stress, and alteration of ER $Ca^{2+}$ storage. The clinically approved bortezomib and carfilzomib are proteasome inhibitors that interfere with protein degradation, enhancing ER stress. Moreover, ROS generation and proteasome inhibition are reported as the main mechanisms of action of copper complexes [13]. Tardito et al. reported a thioxotriazole copper(II) complex capable of inducing UPR via inhibition of the ubiquitin proteasome system. Gene expression profiling showed that the complex up-regulated genes related to the unfolded protein response. Functional analysis revealed an enrichment of chaperone and unfolded protein binding categories [27]. We have previously reported that CuHL1 inhibits proteasome activity [22] and that the proteomic analysis showed a down-regulation of proteasome subunit PSMD4. On the other hand, we have determined that CuHL2 induces a significant increment in the ROS levels [23]. These mechanisms could lead to ER stress and accumulation of unfolded proteins that could explain the up-regulation of HSPs with both complexes.

When we analyzed the down-regulated proteins, we found more differences in GO terms between the two treatments. This is due to a lower proportion of common proteins between CuHL1 and CuHL2 among down-regulated proteins. Shared proteins represent 44% and 45% of down-regulated proteins for CuHL1 and CuHL2, respectively. Meanwhile, the shared up-regulated proteins represent 50% and 61% for CuHL1 and CuHL2, respectively. The only biological process in common is the "Organic substance metabolic process". After CuHL1 treatment, down-regulated proteins were enhanced in other metabolic processes, such as the "Small-molecule metabolic process", "Oxidation–reduction process", and "Carboxylic acid metabolic process".

On the other hand, CuHL2 presents biological processes related to DNA replication and repair. This difference is replicated when we analyzed the Cellular Component. Proteins down-regulated with CuHL2 are found in the "Chromosome telomeric region", "CMG complex", and "MCM complex", which are components related to DNA replication. In a previous work, we demonstrated that CuHL2 is capable of interacting with DNA and cause damage [24]. This could be the reason for the inhibition of proteins related to DNA replication.

### 2.4. Protein–Protein Interaction Analysis

The STRING v11.5 database was used to perform Protein–protein interaction (PPI) analysis to evaluate the interactions between the differentially expressed proteins in response to treatment for both copper complexes. In these networks, the nodes represent proteins, and the edges represent the interactions between the two proteins, whereby the

line thickness between two nodes indicates the strength of data support. For all PPI networks, Markov Cluster Algorithm (MCL) clustering was performed to identify significant protein–protein interaction clusters formed among differentially expressed proteins.

Figure 4 displays the networks generated for up-regulated proteins after treatment with CuHL1 and CuHL2. In both networks, prominent interaction clusters were generated containing HSPs and co-chaperones proteins: BAG3, CHORDC1, DNAJA1, DNAJB1, HSPA1B, and HSPH1 for CuHL1; AHSA1, BAG3, CHORDC1, DNAJA1, DNAJB1, HSPA1B, HSPA6, and HSPH1 for CuHL2. These clusters correlate with the enriched biological processes found in GO analysis.

Both down-regulated networks (Figure 5) display TP53 as a central node. The TP53 tumor suppressor gene encodes the p53 protein, a transcription factor that is crucial for proper control of cell cycle progression, senescence, apoptosis, DNA repair, and genome maintenance among other important functions [28]. The TP53 gene is the most frequent target for mutation in tumors, mutated in over half of all cancers [29]. Moreover, TP53 mutations are highly frequent and one of the key driving factors in triple-negative breast cancer [30]. There are TP53 mutations that result in a "loss of function" that eliminates the tumor suppressing effects of p53. However, many mutations to TP53 are "gain-of-function" (GOF) mutations that can acquire oncogenic properties, augmented invasiveness, metastasis, and recurrence of cancer [31,32]. The expression of mutant p53 in preclinical breast cancer models showed a correlation with increased survival, migration, invasion, and metastasis [30,32,33]. Most mutant p53s are expressed at very high levels in cancer cells, so the degradation or inhibition of their activity can be considered promising therapeutic mechanisms [34]. Particularly, MDA-MB-231 cells present a highly expressed GOF mutant p53. It has been demonstrated that a reduction of mutant p53 can induce apoptosis in MDA-MB-231 cells [35]. Therefore, the down-regulation of mutant p53 is one of the most important antitumor mechanisms of action found for CuHL1 and CuHL2.
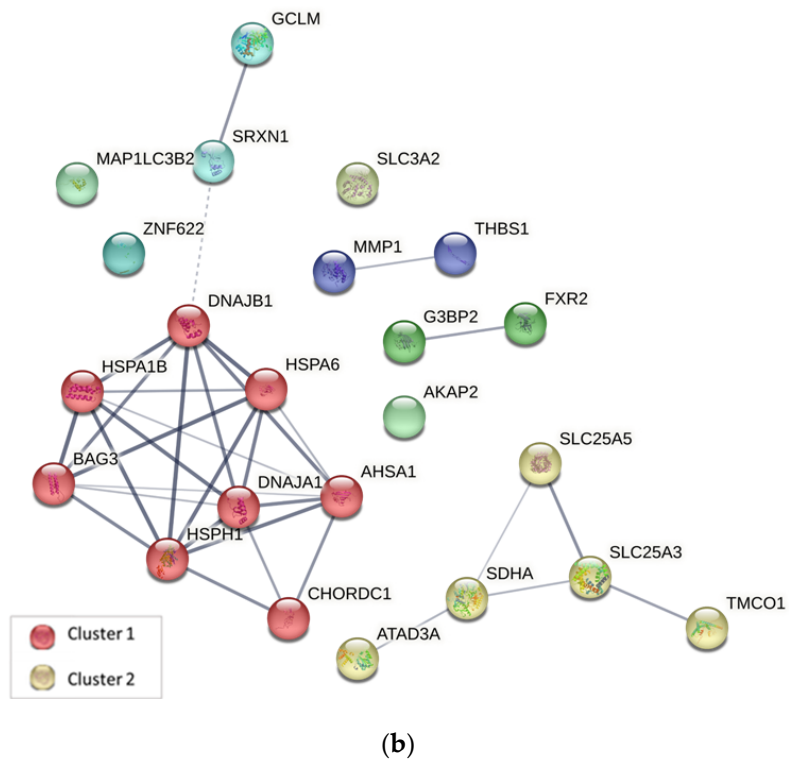


(**a**)

**Figure 4.** *Cont.*

(**b**)
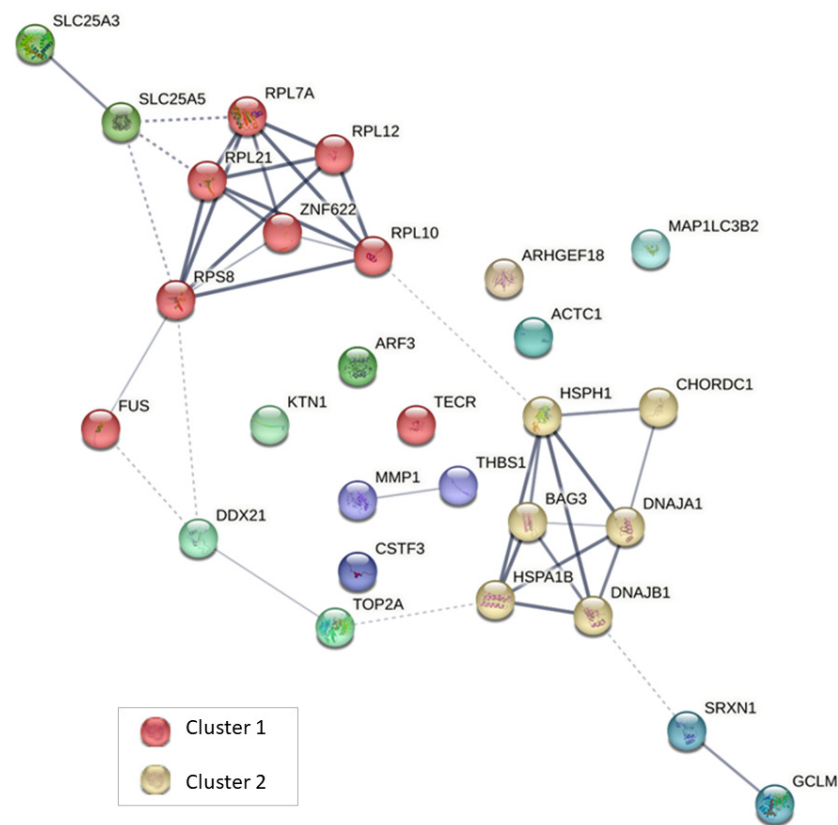
**Figure 4.** Interaction network for up-regulated proteins of MDA-MB-231 cells in response to treatment with (**a**) CuHL1 and (**b**) CuHL2 generated using the STRING v11.5 database. The thickness of the line indicates the degree of confidence of the interaction. A variety of interaction sources were included into the search strategy, such as text mining, experiment record, database record, coexpression, neighborhood, gene fusion, and co-occurrence.
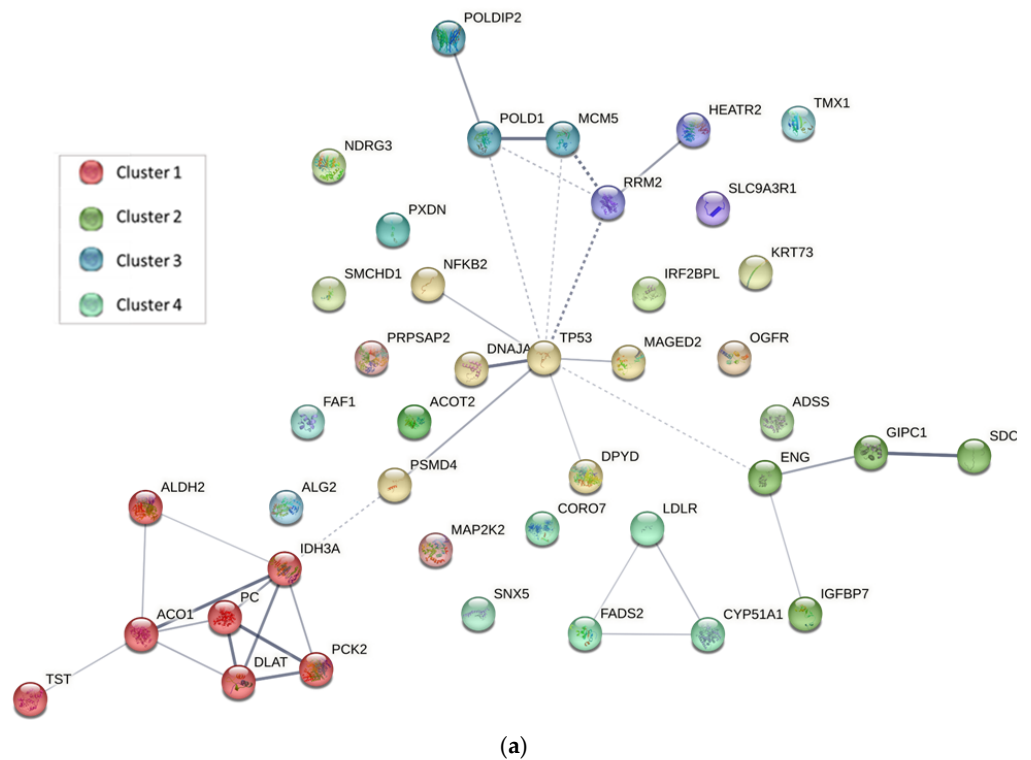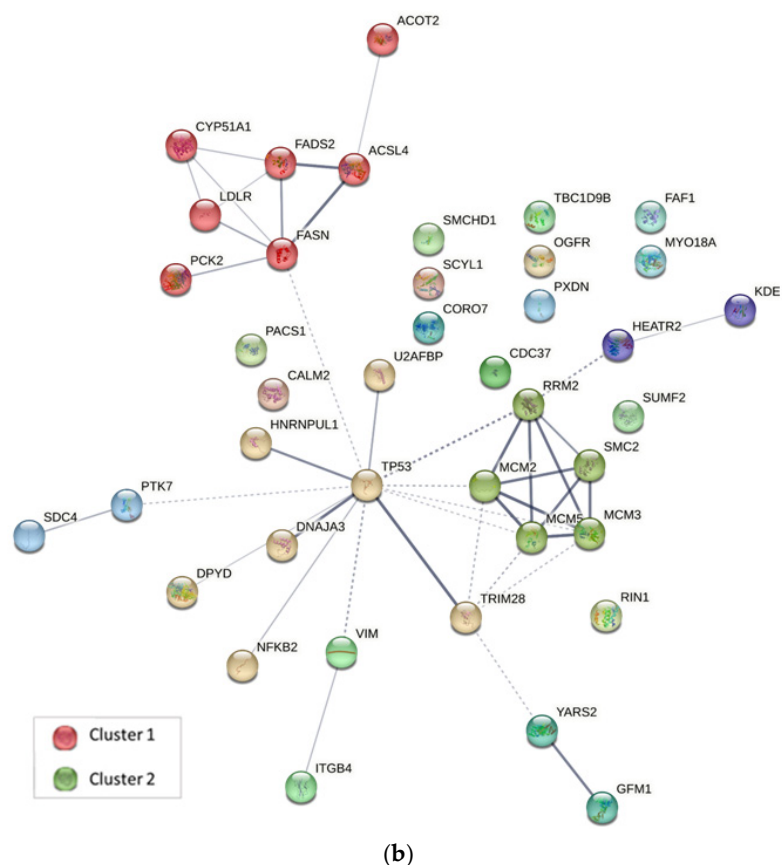


(**a**)

**Figure 5.** *Cont.*

**(b)**

**Figure 5.** Interaction network for down-regulated proteins of MDA-MB-231 cells in response to treatment with (**a**) CuHL1 and (**b**) CuHL2 generated using the STRING v11.5 database. The thickness of the line indicates the degree of confidence of the interaction. A variety of interaction sources were included into the search strategy, such as text mining, experiment record, database record, coexpression, neighborhood, gene fusion, and co-occurrence.

Another similarity in both down-regulated networks is the presence of clusters related to lipid metabolism. Figure 4b presents a cluster form with CYP51A1, FADS2, and LDLR; while the cluster in Figure 3d includes proteins ACOT2, ACSL4, CYP51A1, FADS2, FASN, LDLR, and PCK2. Altered lipid metabolism is a recognized factor in cancer metabolism. Tumor cells tend to increase the novo lipogenesis, lipid uptake, and storage, which leads to an increment in source material for the biogenesis of cell membranes, as well as in energy supplies via β-oxidation of fatty acids, and in an increase in the lipid signaling molecules that mediate oncogenic pathways [36]. This lipid metabolism dysregulation helps to promote tumor growth, metastatic spread, and therapy resistance [37]. The up-regulation of lipogenic enzymes has been reported in several cancers including breast, prostate, colorectal, ovarian, gastrointestinal, and lung cancer [38,39]. Consequently, targeting-altered lipid metabolism pathways have been studied as a promising anticancer therapy.

One of the most down-regulated proteins after treatment with CuHL1 was Lanosterol 14-alpha demethylase (CYP51A1). This protein catalyzes one of the key steps in cholesterol biosynthesis and is usually overexpressed in tumor cells [40]. In fact, Kerber et al. demonstrated that de novo cholesterol synthesis was blocked when CYP51A1 was knocked-out [41]. Furthermore, the presence of a lanosterol 14-alpha demethylase inhibitor led to the induction of apoptosis in cancer cells [42]. In this sense, several pre-clinical and clinical studies have focused on targeting cholesterol metabolism as a treatment for various cancers [43]. The strategies include aiming for cholesterol biosynthesis pathways, as well as the exogenous-sterol uptake. For example, current clinical trials have demonstrated

the protective effect in breast cancer of drugs that inhibit the mevalonate pathway such as statins and Zoledronate [44].

On the other hand, many cancer cells exhibit an overexpression of LDLR, which facilitates the rapid uptake of LDL cholesterol and contributes to the accumulation of lipid components [45,46]. Thus, the downregulation or inhibition of LDLR affects cholesterol uptake and could increase the efficacy of chemotherapeutic drugs. Guillaumond et al. demonstrated that the shRNA silencing of LDLR reduced the cholesterol uptake and diminished the proliferation of pancreatic cancer cells [47]. For breast cancer, Gallagher et al. showed that elevated LDLR expression and high LDL levels are significant for tumor growth and that silencing LDLR in TNBC cells increases cell death and reduces the growth of tumors [48]. Proteomics showed that LDLR was down-regulated after treatment with both complexes in MDA-MB-231 cells. This TNBC cell line presents higher expression levels of LDLR compared to the estrogen-receptor-positive MCF7, or the non-tumorigenic MCF-10A cell lines [48].

Other proteins related to lipid metabolism were down-regulated by CuHL1 and CuHL2. They are key enzymes that participate in fatty acid metabolism, such as fatty acid synthase (FASN), fatty acid desaturase (FADS2), and long-chain fatty acid synthase (ACSL4). Fatty acid synthesis and palmitoleic acid generation are enhanced and play an essential role in cancer growth [36]. FASN and ACSL4 are highly expressed in many cancers including breast cancer [49,50], thus making them an attractive target for inhibiting cancer cell proliferation. In this sense, Cui et al. showed that inhibiting FAS by inhibitors or shRNAs induces apoptosis in breast cancer cells [51]. Another FASN inhibitor, Fasnall, was able to inhibit breast cancer cell growth, induce apoptosis, and showed potent in vivo antitumor activity against breast cancer, alone and combined with carboplatin [52]. Similarly, ACSL4 knockdown inhibited the cell proliferation of several cancer cell lines [53,54]. In breast cancer, it was demonstrated that ACSL4 targeting increased the efficacy of Triacsin C, as combined treatment with ACSL4 inhibition resulted in synergistic antitumor effects [55]. Overall, the down-regulation of these proteins by CuHL1 and CuHL2 could lead to a beneficial decrease in lipid synthesis and metabolism, which is a novel and interesting effect for a copper metallodrug.

CuHL1 presented a cluster in the down-regulated network that includes proteins also related to cell metabolism, specifically associated with the tricarboxylic acid (TCA) cycle and pyruvate metabolism. The cluster forms with all mitochondrial proteins: ACO1, ALDH2, DLAT, IDH3A, PC, PCK2, and TST. This cluster correlates with the enriched metabolic processes in GO functional analysis: "Small-molecule metabolic process", "Oxidation–reduction process", and "Carboxylic acid metabolic process". CuHL1 could generate the inhibition of mitochondrial metabolism. Traditionally, "the Warburg effect" hypothesizes that most cancer cells rely on aerobic glycolysis to engender the energy needed for cellular activity, rather than mitochondrial oxidative phosphorylation [56]. However, recent studies indicate that active mitochondrial metabolism is necessary for tumor growth as it provides key metabolites for macromolecule synthesis and generates oncometabolites to sustain the phenotype of cancer cells [57]. In particular, recent studies have shown that TNBCs have an altered metabolic profile, characterized by the elevated uptake and utilization of glucose, glutamine, and TCA cycle intermediates in addition to increased fatty acid $\beta$-oxidation [58–60]. As a consequence, the down-regulating effect of CuHL1 on several proteins related to mitochondrial metabolism could be beneficial for breast cancer therapy.

Moreover, Tsvetkov et al. recently defined a new copper-dependent form of regulated cell death related to mitochondrial metabolism called cuproptosis. In this cell-death mechanism, excess copper binds to lipoylated enzymes of the TCA cycle, resulting in lipoylated protein aggregation that leads to proteotoxic stress and ultimately cell death [61]. One of the lipoylated proteins that can bind to copper is DLAT, which is down-regulated after treatment with CuHL1. The decreased expression of DLAT could be the result of protein oligomerization caused by copper binding. In fact, Zhou et al. reported a copper nanoplatform that induces cuproptosis and generates the same down-regulating effect in DLAT [62]. Furthermore, the proteotoxic stress caused by protein oligomerization leads

to the induction of HSP70, whose expression is increased by both complexes. This could indicate that CuHL1 is able to promote cuproptosis as a cell-death mechanism.

Another important cluster in the CuHL2 down-regulated network includes proteins that participate in DNA replication: MCM2, MCM3, MCM5, RRM2, and SMC2. These proteins are responsible for the related GO terms that were mentioned before. Nevertheless, in this analysis, we found that CuHL1 also has a cluster formed with proteins that participate in DNA replication: MCM5, POLD1, and POLDIP2. We have demonstrated, in in silico and in vitro studies, that both complexes were able to interact with DNA and produce damage in the macromolecule [22,23]. The down-regulation of minichromosome maintenance (MCM) proteins is present in both CuHL1 and CuHL2 treatments. The MCM protein family plays a key role in eukaryotic DNA replication. The MCM complex is a DNA replication licensing factor that controls the once-per-cell cycle DNA replication [63]. Dysregulation of the MCM complex has been associated with the occurrence and progression of many tumors [64]. Moreover, overexpression of MCM has been detected in various cancer cells, including breast cancer [65]. Additionally, CuHL1 presented a down-regulation of POLD1. The DNA polymerase delta (POLD) family is involved in DNA replication and is an important mediator of DNA repair during chromosome replication [66]. Mutation in POLD can be associated with cancer development and it was demonstrated that POLD1 is able to affect cell cycle progression and promote cancer cell proliferation [67]. In breast cancer, gene and protein expression levels of POLD1 are elevated [68]. Moreover, survival analysis demonstrated an association of increased POLD1 levels with poor disease-free survival, late-stage cases, and the presence of TNBC [69]. In this sense, several studies report that the down-regulation of POLD1 in breast cancer cells suppressed cell cycle progression and cell proliferation and promoted apoptosis [69,70].

In order to analyze the shared mechanisms of CuHL1 and CuHL2, we performed a PPI network analysis utilizing only the common proteins between both treatments.

Figure 6a displays the network generated for the shared up-regulated proteins. The interaction cluster generated includes HSPs and co-chaperone proteins: BAG3, CHORDC1, DNAJA1, DNAJB1, HSPA1B, and HSPH1. This cluster demonstrates the shared mechanism of ER stress and UPR induction for both complexes.
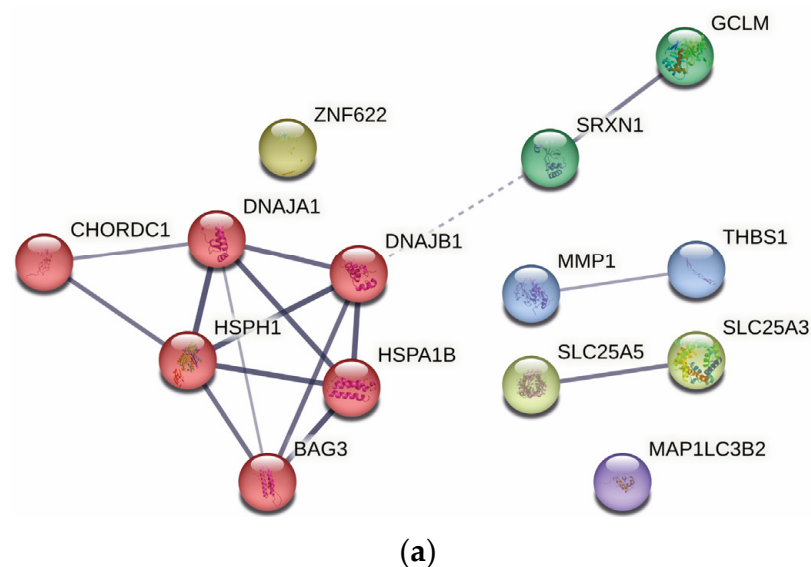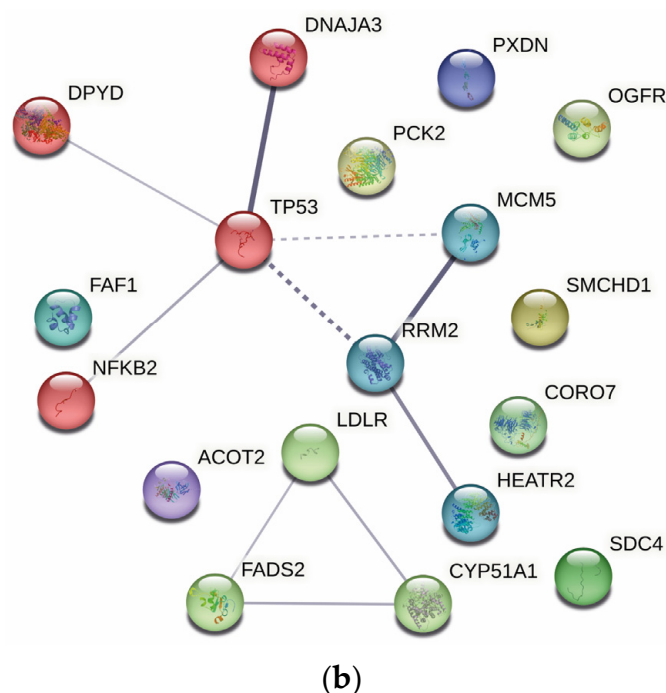


(a)

**Figure 6.** *Cont.*

**(b)**

**Figure 6.** Interaction network for shared proteins between CuHL1 and CuHL2. (**a**) Up-regulated proteins; (**b**) Down-regulated proteins. Generated using the STRING v11.5 database. The thickness of the line indicates the degree of confidence of the interaction. A variety of interaction sources were included into the search strategy, such as text mining, experiment record, database record, coexpression, neighborhood, gene fusion, and co-occurrence.

The down-regulated network (Figure 6b) presents the p53 central node. Moreover, a cluster related to lipid and cholesterol metabolism is shown. The cluster includes the proteins: LDLR, CYP51A1, and FADS2. This way, other shared mechanisms between CuHL1 and CuHL2 include the down-regulation of GOF-p53 and proteins involved in lipid metabolism.

*2.5. Ingenuity Pathway Analysis*

Finally, the ingenuity pathway analysis (IPA) bioinformatics tool was run to evaluate the most affected canonical pathways after treatment with both complexes. The over-represented canonical pathways are reported in Tables 3 and 4.

**Table 3.** Ingenuity canonical pathways associated with the differentially expressed proteins in CuHL1-treated cells.

| Canonical Pathways | *p*-Value | Proteins |
|---|---|---|
| EIF2 Signaling | $4.78 \times 10^{-6}$ | ACTC1, MAP2K2, RPL10, RPL12, RPL21, RPL7A, RPS8 |
| Unfolded protein response | $6.97 \times 10^{-6}$ | DNAJA1, DNAJA3, DNAJB1, HSPA1A/HSPA1B, HSPH1 |
| Induction of Apoptosis by HIV1 | $4.09 \times 10^{-5}$ | NFKB2, SLC25A3, SLC25A5, TP53 |
| NRF2-mediated Oxidative Stress Response | $7.13 \times 10^{-5}$ | ACTC1, DNAJA1, DNAJA3, DNAJB1, GCLM, MAP2K2 |
| BAG2 Signaling Pathway | $1.12 \times 10^{-4}$ | HSPA1A/HSPA1B, NFKB2, PSMD4, TP53 |
| Aldosterone Signaling in Epithelial Cells | $1.39 \times 10^{-4}$ | DNAJA1, DNAJB1, HSPA1A/HSPA1B, HSPH1, MAP2K2 |
| Bladder Cancer Signaling | $3.87 \times 10^{-4}$ | MAP2K2, MMP1, THBS1, TP53 |
| Cell Cycle Control of Chromosomal Replication | $6.08 \times 10^{-4}$ | MCM5, POLD1, TOP2A |

**Table 3.** *Cont.*

| Canonical Pathways | p-Value | Proteins |
| --- | --- | --- |
| Protein Ubiquitination Pathway | $1.30 \times 10^{-3}$ | DNAJA1, DNAJB1, HSPA1A/HSPA1B, HSPH1, PSMD4 |
| Ribonucleotide Reductase Signaling Pathway | $1.61 \times 10^{-3}$ | NFKB2, RRM2, THBS1, TP53 |
| HIF1α Signaling | $3.34 \times 10^{-3}$ | HSPA1A/HSPA1B, MAP2K2, MMP1, TP53 |
| Apoptosis Signaling | $3.61 \times 10^{-3}$ | MAP2K2, NFKB2, TP53 |
| Autophagy | $3.82 \times 10^{-3}$ | MAP1LC3B2, MAP2K2, NFKB2, TP53 |
| HER-2 Signaling in Breast Cancer | $4.56 \times 10^{-3}$ | ARF3, MAP2K2, NFKB2, TP53 |

**Table 4.** Ingenuity canonical pathways associated with the differentially expressed proteins in CuHL2-treated cells.

| Canonical Pathways | p-Value | Proteins |
| --- | --- | --- |
| Unfolded protein response | $1.28 \times 10^{-7}$ | DNAJA1, DNAJA3, DNAJB1, HSPA6, HSPA1A/HSPA1B, HSPH1 |
| Sirtuin Signaling Pathway | $1.10 \times 10^{-5}$ | MAP1LC3B2, NFKB2, PCK2, SDHA, SLC25A5, TP53, TRIM28 |
| Induction of Apoptosis by HIV1 | $2.51 \times 10^{-5}$ | NFKB2, SLC25A3, SLC25A5, TP53 |
| BAG2 Signaling Pathway | $6.90 \times 10^{-5}$ | HSPA6, HSPA1A/HSPA1B, NFKB2, TP53 |
| Aldosterone Signaling in Epithelial Cells | $7.73 \times 10^{-5}$ | DNAJA1, DNAJB1, HSPA6, HSPA1A/HSPA1B, HASPH1 |
| HIF1α Signaling | $2.10 \times 10^{-4}$ | HSPA6, HSPA1A/HSPA1B, MMP1, TP53, VIM |
| Autophagy | $2.50 \times 10^{-4}$ | CALM1, MAP1LC3B2, NFKB2, SLC3A2, TP53 |
| LXR/RXR Activation | $3.01 \times 10^{-4}$ | CYP51A1, FASN, LDLR, NFKB2 |
| Cell Cycle Control of Chromosomal Replication | $4.24 \times 10^{-4}$ | MCM2, MCM3, MCM5 |
| Ribonucleotide Reductase Signaling Pathway | $1.02 \times 10^{-3}$ | NFKB2, RRM2, THBS1, TP53 |
| Immunogenic Cell Death Signaling Pathway | $1.69 \times 10^{-3}$ | HSPA6, HSPA1A/HSPA1B, NFKB2 |
| PI3K/AKT Signaling | $1.85 \times 10^{-3}$ | CDC37, ITGB4, NFKB2, TP53 |
| NRF2-mediated Oxidative Stress Response | $3.41 \times 10^{-3}$ | DNAJA1, DNAJA3, DNAJB1, GCLM |
| Inhibition of Angiogenesis by TSP1 | $3.55 \times 10^{-3}$ | THBS1, TP53 |
| MYC-Mediated Apoptosis Signaling | $7.56 \times 10^{-3}$ | NFKB2, TP53 |
| FAT10 Cancer Signaling Pathway | $7.56 \times 10^{-3}$ | NFKB2, TP53 |

In correlation with the results of up-regulated proteins analysis, both complexes displayed an alteration in stress-response pathways such as "Unfolded protein response", "NRF2-mediated oxidative stress response" [71], and "Autophagy". The latter can be positively stimulated by the UPR program because, under ER stress conditions, ER produces several signals that stimulate autophagy [72]. Moreover, CuHL1 presented an enrichment of the "Protein ubiquitination pathway" and "EIF2 signaling", which is involved in one of the UPR pathways [25].

Molecular pathways related to cell death were enhanced. Both complexes displayed alterations in "Induction of Apoptosis by HIV1". "Apoptosis signaling" was also altered by CuHL1. Meanwhile, CuHL2 displayed an enhancement of "Immunogenic cell death" (ICD). ICD is a form of cell death where the dying cancer cells stimulate immune cells to actively seek and destroy them. ICD is characterized by the emission of a class of the danger-associated

molecular patterns (DAMPs) family, which functions as "find me" and "eat me" signals to the tumor-associated immune cells. The key DAMPs include the release of adenosine triphosphate (ATP), high-mobility group protein B1 (HMBG1), and exposed molecules on the outer membrane such as CRT (CRT) and heat-shock proteins (Hsp90 and Hsp70) [73]. In this sense, both complexes have Hsp70 proteins as the most up-regulated protein. Moreover, the ability of cancer therapies to induce ICD depends on their ability to induce ER stress and ROS production. ROS-based ER stress is an essential component to trigger DAMPs expression and the intracellular danger signaling pathways [74]. Redox stress induction is the principal mode of action for several anticancer copper complexes. Kaur et al. reported a Cu(II) complex with a Schiff base ligand that is capable of inducing ICD in breast cancer stem cells through elevation of ROS levels and induction of ER stress [75].

Angiogenesis was another process affected by both complexes, as seen by the alteration of "Inhibition of Angiogenesis by TSP1" and "HIFa signaling". In this sense, CuHL1 presented a cluster in the down-regulated network (Figure 4b) related to vascular endothelial growth factor (VEGF) signaling and angiogenesis, formed with proteins ENG, GIPC1, IGFBP7, and SDC4. Angiogenesis is essential for breast cancer progression and dissemination. Several molecular pathways are known to drive angiogenic switches in cancer cells [76]. Hence, the inhibition of pro-angiogenic pathways is a promising therapeutic alternative. There are numerous clinical and pre-clinical studies on targeting angiogenic pathways in breast cancer [77].

Finally, DNA replication and repair pathways were also affected, as seen in the GO functional analysis and PPI networks. Both complexes displayed an alteration of "Cell cycle control of chromosomal replication" and "Ribonucleotide reductase (RR) signaling pathway". RR catalyzes the reduction of ribonucleotides to their corresponding deoxyribonucleotides, so RR is essential for DNA replication and repair [78]. The expression of subunit RRM2 is dysregulated in multiple cancer types, including breast cancer. Particularly, the MDA-MB-231 cell line presents an increased expression of RRM2 [79].

## 3. Materials and Methods

### 3.1. Synthesis, Identification, and Preparation of CuHL1 and CuHL2

Both copper(II) compounds were obtained following the procedure defined in our previous manuscripts [21,23].

Fresh stock 20 mM solutions of the complexes were prepared in dimethylsulfoxide (DMSO) and forward-diluted according to the concentrations used in each experiment. The maximum concentration of DMSO was maintained at 0.5% to avoid the toxic effects of this solvent on the cells.

### 3.2. Cell Culture

MDA-MB-231 breast cancer cells were grown in Dulbecco's modified Eagle's medium Nutrient Mixture F12 (DMEM F12) with 10% fetal bovine serum (FBS), 100 IU/mL of penicillin, and 100 µg/mL of streptomycin at 37 °C in a 5% $CO_2$ atmosphere.

### 3.3. Protein Sample Preparation

For sample preparation, MDA-MB-231 cells were seeded in a 6-well dish, allowed to attach for 24 h, and treated with 1 µM of the complex at 37 °C. Triplicates of each condition were used. Total protein was extracted from MG-63 cells after 24 h. Briefly, cells were homogenized in RIPA lysis buffer containing a protease inhibitor cocktail. Then, total protein was collected through centrifugation at $12,000 \times g$ for 20 min at 4 °C, and protein concentration was determined using the BCA protein assay.

### 3.4. Protein Identification and Mass Spectrometry

Samples were sent to the Center for Chemical and Biological Studies by Mass Spectrometry (CEQUIBIEM) for Label-Free Quantification analysis. In brief, samples were reduced with DTT, alkylated with iodoacetamide, and followed by trypsin digestion. Sam-

ples were lyophilized by Speed Vac and resuspended in 0.1% trifluoroacetic acid. Then, liquid chromatography was performed with the nanoHPLC Easy nLC 1000 (Thermo Scientific, Waltham, MA, USA) coupled to a mass spectrometer with Orbitrap technology (Thermo Scientific, Waltham, MA, USA), which allows separation and further identification of the peptides.

Analysis of the spectra obtained by the mass spectrometer was performed using the Proteome Discoverer search engine with the Homo sapiens database. For the search, the following parameters were set: trypsin was used as the cleavage protease; two missed cleavages were allowed; the precursor peptide mass tolerance was set at 10 ppm while the fragment mass tolerance was 0.05 Da; carbamidomethylation (C) was set as a fixed modification; the variable modification was set to oxidation; the minimum identification criteria required a minimum of 2 peptides per protein.

Statistical analysis for differentially expressed proteins was performed using the software Perseus v.1.6.6.0. The *t*-test was used to compare protein abundance averages between treatment and control groups. Differentially expressed proteins were identified when the *t*-test *p* value < 0.05 and there was an increase or decrease in the protein level of 2-fold or more.

### 3.5. Bioinformatics Analysis

#### 3.5.1. Functional GO Enrichment Analysis

The differentially expressed proteins were used to perform Gene Ontology (GO) enrichment analysis with the Search Tool for the Retrieval of Interacting Genes (STRING) enrichment API method (https://string-db.org, accessed on 12 December 2022). For that, the up- and down-regulated protein IDs were submitted for Homo sapiens and were categorized according to their molecular function, biological process, and cellular component. For each of the different GO categories, the False Discovery Rate and Bonferroni-corrected *p*-values were calculated.

#### 3.5.2. Protein–Protein Interaction Analysis

The STRING v11.5 database was used to predict functional interactions between differentially expressed proteins and to map the protein–protein interaction networks (http://string-db.org, accessed on 12 December 2022). Protein IDs were submitted into the multiple protein analysis, and interaction sources were selected: text mining, experiments, databases, co-expression, neighborhood, gene fusion, and co-occurrence. A default medium confidence threshold (0.4) was used to define protein–protein interactions. MCL clustering (inflation parameter 3) was applied to the analysis to identify protein groups with similar interactions.

#### 3.5.3. Ingenuity Pathway Analysis

Pathway analysis was evaluated using Ingenuity Pathway Analysis (IPA). The dataset for each complex, combining up-regulated and down-regulated proteins, was uploaded into the QIAGEN IPA (QIAGEN Inc., Venlo, Netherlands) system for core analysis. IPA was performed to identify the most significant canonical pathways. The significance values (*p*-value) for the canonical pathways were calculated by the right-tailed Fisher's Exact Test.

### 4. Conclusions

In this study, we conducted a label-free quantitative proteomic analysis of MDA-MB-231 cells treated with CuHL1 and CuHL2 to provide insight into the molecular mechanism of these copper complexes in TNBC cells. Bioinformatic and functional analysis revealed similar modes of action between both complexes. CuHL1 and CuHL2 treatment generated an increment of proteins involved in ER stress and UPR, as well as the down-regulation of proteins related to DNA replication and repair. One of the most important antitumor mechanisms of action found for CuHL1 and CuHL2 was the down-regulation of GOF-mutant p53. Additionally, we found a novel and interesting effect for a copper metallodrug, which was the down-regulation of proteins related to lipid synthesis and metabolism that could lead

to a beneficial decrease in lipid levels. However, further functional studies are required to understand the specific mechanisms underlying the antitumoral effects of CuHL1 and CuHL2. It will be necessary to carry out experimental validations based on biochemical and other functional experiments, which go beyond the aim of the present work.

## Abbreviations

ACLSL4: Long-chain-fatty-acid CoA ligase 4; ACO1: Aconitase 1; AHSA1: Activator of HSP90 ATPase Activity 1; ALDH2: Aldehyde dehydrogenase; API: Application programming interface; ATP: Adenosine triphosphate; CHORDC1: Cysteine And Histidine Rich Domain Containing 1; CMG: Cdc45-Mcm2-7-GINS; CRT: Calreticulin; CYP1A1: Lanosterol 14-alpha demethylase; DAMPs: Danger-associated molecular patterns; DLAT: Dihydrolipoyllysine-residue acetyltransferase component of pyruvate dehydrogenase complex; DMEM F12: Dulbecco's modified Eagle's medium Nutrient Mixture F12; DMSO: Dimethylsulfoxide; DNAJA1: DnaJ homolog subfamily A member 1; DNAJB1: DnaJ homolog subfamily B member 1; EIF2: Eukaryotic Initiation Factor 2; ER: Endoplasmic reticulum; FASDS2: Fatty acid desaturase 2; FASN: Fatty Acid Synthase; FAT10: Human leukocyte antigen F adjacent transcript 10; FBS: Fetal bovine serum; GO: Gene Ontology; GOF: Gain of function; GSH: Glutation; HIF$\alpha$: Hypoxia-inducible factor $\alpha$-subunits; HMBG1: High-mobility group protein B1; HSP: Heat shock protein; HSPA1B: Heat shock 70 kDa protein 1B; HSPH1: Heat shock protein 105 kDa; IC50: Half-maximal inhibitory concentration; ICD: Immunogenic cell death; IDH3A: Isocitrate dehydrogenase; IPA: Ingenuity pathway analysis; LDL: Low-density lipoprotein; LDLR: Low-density lipoprotein Receptor; LXR/RXR: Liver X Receptor-Retinoid X Receptor; MCL: Markov Cluster Algorithm; MCM: Minichromosome maintenance; MCM2: DNA replication licensing factor 2; MCM3: DNA replication licensing factor 3; MCM5: DNA replication licensing factor 5; NRF2: Nuclear factor erythroid 2–related factor 2; PC: Pyruvate carboxylase; PCK2: Phosphoenolpyruvate carboxykinase; POLD1: DNA polymerase; POLDIP2: Polymerase delta-interacting protein 2; PPI: DNA polymerase; ROS: Reactive oxygen species; RR: Ribonucleotide reductase; RRM2: Ribonucleoside-diphosphate reductase subunit M2; SMC2: Structural maintenance of chromosomes protein 2; STRING: Search Tool for the Retrieval of Interacting Genes; TCA cycle: Tricarboxylic acid cycle; TNBC: Triple-Negative Breast Cancer; TP53: Cellular tumor antigen p53; TST: Thiosulfate sulfurtransferase; UPR: Unfolded protein response; VEGF: Vascular endothelial growth factor.

## References

1. Torre, L.A.; Bray, F.; Siegel, R.L.; Ferlay, J.; Lortet-Tieulent, J.; Jemal, A. Global cancer statistics, 2012. *CA Cancer J. Clin.* **2015**, *65*, 87–108. [CrossRef] [PubMed]
2. Alanazi, I.O.; Khan, Z. Understanding EGFR Signaling in Breast Cancer and Breast Cancer Stem Cells: Overexpression and Therapeutic Implications. *Asian Pac. J. Cancer Prev.* **2016**, *17*, 445–453. [CrossRef] [PubMed]
3. Wen, S.; Manuel, L.; Doolan, M.; Westhuyzen, J.; Shakespeare, T.P.; Aherne, N.J. Effect of Clinical and Treatment Factors on Survival Outcomes of Triple Negative Breast Cancer Patients. *Breast Cancer Targets Ther.* **2020**, *12*, 27–35. [CrossRef]
4. So, J.Y.; Ohm, J.; Lipkowitz, S.; Yang, L. Triple negative breast cancer (TNBC): Non-genetic tumor heterogeneity and immune microenvironment: Emerging treatment options. *Pharmacol. Ther.* **2022**, *237*, 108253. [CrossRef]
5. Al-Mahmood, S.; Sapiezynski, J.; Garbuzenko, O.B.; Minko, T. Metastatic and triple-negative breast cancer: Challenges and treatment options. *Drug Deliv. Transl. Res.* **2018**, *8*, 1483–1507. [CrossRef] [PubMed]
6. Lin, C.Y.; Barry-Holson, K.Q.; Allison, K.H. Breast cancer stem cells: Are we ready to go from bench to bedside? *Histopathology* **2016**, *68*, 119–137. [CrossRef] [PubMed]
7. Vojtek, M.; Marques, M.P.M.; Ferreira, I.M.P.L.V.O.; Mota-Filipe, H.; Diniz, C. Anticancer activity of palladium-based complexes against triple-negative breast cancer. *Drug Discov. Today* **2019**, *24*, 1044–1058. [CrossRef]
8. Hongthong, K.; Ratanaphan, A. BRCA1-Associated Triple-Negative Breast Cancer and Potential Treatment for Ruthenium-Based Compounds. *Curr. Cancer Drug Targets* **2016**, *16*, 606–617. [CrossRef]
9. Nhukeaw, T.; Temboot, P.; Hansongnern, K.; Ratanaphan, A. Cellular responses of BRCA1-defective and triple-negative breast cancer cells and in vitro BRCA1 interactions induced by metallo-intercalator ruthenium (II) complexes containing chloro-substituted phenylazopyridine. *BMC Cancer* **2014**, *14*, 73. [CrossRef]
10. Boodram, J.N.; Mcgregor, I.J.; Bruno, P.M.; Cressey, P.B.; Hemann, M.T.; Suntharalingam, K. Breast Cancer Stem Cell Potent Copper (II)-Non-Steroidal Anti-Inflammatory Drug Complexes. *Angew. Chem.-Int. Ed.* **2016**, *55*, 2845–2850. [CrossRef]
11. Denoyer, D.; Masaldan, S.; La Fontaine, S.; Cater, M.A. Targeting copper in cancer therapy: "Copper That Cancer". *Metallomics* **2015**, *7*, 1459–1476. [CrossRef] [PubMed]
12. Santini, C.; Pellei, M.; Gandin, V.; Porchia, M.; Tisato, F.; Marzano, C. Advances in copper complexes as anticancer agents. *Chem. Rev.* **2014**, *114*, 815–862. [CrossRef] [PubMed]
13. Balsa, L.M.; Baran, E.J.; León, I.E. Copper complexes as antitumor agents: In vitro and in vivo evidences. *Curr. Med. Chem.* **2023**, *30*, 510–557. [CrossRef]
14. Leon, I.; Cadavid-Vargas, J.; Di Virgilio, A.; Etcheverry, S. Vanadium, Ruthenium and Copper Compounds: A New Class of Nonplatinum Metallodrugs with Anticancer Activity. *Curr. Med. Chem.* **2016**, *24*, 112–148. [CrossRef]
15. Laws, K.; Bineva-Todd, G.; Eskandari, A.; Lu, C.; O'Reilly, N.; Suntharalingam, K. A Copper(II) Phenanthroline Metallopeptide That Targets and Disrupts Mitochondrial Function in Breast Cancer Stem Cells. *Angew. Chem. Int. Ed.* **2018**, *57*, 287–291. [CrossRef] [PubMed]
16. Balsa, L.M.; Ruiz, M.C.; Santa Maria de la Parra, L.; Baran, E.J.; León, I.E. Anticancer and antimetastatic activity of copper (II)-tropolone complex against human breast cancer cells, breast multicellular spheroids and mammospheres. *J. Inorg. Biochem.* **2019**, *204*, 110975. [CrossRef] [PubMed]
17. Sîrbu, A.; Palamarciuc, O.; Babak, M.V.; Lim, J.M.; Ohui, K.; Enyedy, E.A.; Shova, S.; Darvasiová, D.; Rapta, P.; Ang, W.H.; et al. Copper (II) thiosemicarbazone complexes induce marked ROS accumulation and promote nrf2-mediated antioxidant response in highly resistant breast cancer cells. *Dalt. Trans.* **2017**, *46*, 3833–3847. [CrossRef]
18. Romo, A.I.B.; Abreu, D.S.; Paulo, T.; Carepo, M.S.P.; Sousa, E.H.S.; Lemus, L.; Aliaga, C.; Batista, A.A.; Nascimento, O.R.; Abruña, H.D.; et al. Hydroxyl Radical Generation and DNA Nuclease Activity: A Mechanistic Study Based on a Surface-Immobilized Copper Thioether Clip-Phen Derivative. *Chem. A Eur. J.* **2016**, *22*, 10081–10089. [CrossRef]
19. Romo, A.I.B.; Carepo, M.P.; Levín, P.; Nascimento, O.R.; Díaz, D.E.; Rodríguez-López, J.; León, I.E.; Bezerra, L.F.; Lemus, L.; Diógenes, I.C.N. Synergy of DNA intercalation and catalytic activity of a copper complex towards improved polymerase inhibition and cancer cell cytotoxicity. *Dalt. Trans.* **2021**, *50*, 11931–11940. [CrossRef]
20. Wang, Y.; Chiu, J.F. Proteomic Approaches in Understanding Action Mechanisms of Metal-Based Anticancer Drugs. *Met. Based Drugs* **2008**, *2008*, 716329. [CrossRef]
21. Rodríguez, M.R.; Balsa, L.M.; Piro, O.E.; Etcheverría, G.A.; García-Tojal, J.; Pis-Diez, R.; León, I.E.; Parajón-Costa, B.P.; González-Baró, A.C. Synthesis, crystal structure, spectroscopic characterization, DFT calculations and cytotoxicity assays of a new cu (II) complex with an acylhydrazone Ligand derived from thiophene. *Inorganics* **2021**, *9*, 9. [CrossRef]
22. Balsa, L.M.; Rodriguez, M.R.; Parajón-Costa, B.S.; González Baró, A.C.; Lavecchia, M.J.; León, I. Anticancer activity and mechanism of action evaluation of an acylhydrazone Cu (II) complex toward breast cancer cells, spheroids and mammospheres. *ChemMedChem* **2022**, *17*, e202100520. [CrossRef] [PubMed]
23. Balsa, L.M.; Ferraresi-Curotto, V.; Lavecchia, M.J.; Echeverría, G.A.; Piro, O.E.; García-Tojal, J.; Pis-Diez, R.; González-Baró, A.C.; León, I.E. Anticancer activity of a new copper (ii) complex with a hydrazone ligand. Structural and spectroscopic characterization, computational simulations and cell mechanistic studies on 2D and 3D breast cancer cell models. *Dalt. Trans.* **2021**, *50*, 9812–9826. [CrossRef]
24. Tiligada, E. Chemotherapy: Induction of stress responses. *Endocr. Relat. Cancer* **2006**, *13*, 115–124. [CrossRef] [PubMed]

25. Oakes, S.A. Endoplasmic reticulum proteostasis: A key checkpoint in cancer. *Am. J. Physiol.-Cell Physiol.* **2017**, *312*, C93–C102. [CrossRef] [PubMed]

26. Walter, P.; Ron, D. The unfolded protein response: From stress pathway to homeostatic regulation. *Science* **2011**, *334*, 1081–1086. [CrossRef] [PubMed]

27. Tardito, S.; Isella, C.; Medico, E.; Marchiò, L.; Bevilacqua, E.; Hatzoglou, M.; Bussolati, O.; Franchi-Gazzola, R. The thioxotriazole copper (II) complex A0 induces endoplasmic reticulum stress and paraptotic death in human cancer cells. *J. Biol. Chem.* **2009**, *284*, 24306–24319. [CrossRef] [PubMed]

28. Lane, D.P. P53, Guardian of the Genome. *Nature* **1992**, *358*, 15–16. [CrossRef]

29. Vogelstein, B.; Lane, D.; Levine, A.J. Surfing the p53 network. *Nature* **2000**, *408*, 307–310. [CrossRef]

30. Walerych, D.; Napoli, M.; Collavin, L.; Del Sal, G. The rebel angel: Mutant p53 as the driving oncogene in breast cancer. *Carcinogenesis* **2012**, *33*, 2007–2017. [CrossRef]

31. Hui, L.; Zheng, Y.; Yan, Y.; Bargonetti, J.; Foster, D.A. Mutant p53 in MDA-MB-231 breast cancer cells is stabilized by elevated phospholipase D activity and contributes to survival signals generated by phospholipase D. *Oncogene* **2006**, *25*, 7305–7310. [CrossRef] [PubMed]

32. Muller, P.A.J.; Caswell, P.T.; Doyle, B.; Iwanicki, M.P.; Tan, E.H.; Karim, S.; Lukashchuk, N.; Gillespie, D.A.; Ludwig, R.L.; Gosselin, P.; et al. Mutant p53 Drives Invasion by Promoting Integrin Recycling. *Cell* **2009**, *139*, 1327–1341. [CrossRef] [PubMed]

33. Adorno, M.; Cordenonsi, M.; Montagner, M.; Dupont, S.; Wong, C.; Hann, B.; Solari, A.; Bobisse, S.; Rondina, M.B.; Guzzardo, V.; et al. A Mutant-p53/Smad Complex Opposes p63 to Empower TGFβ-Induced Metastasis. *Cell* **2009**, *137*, 87–98. [CrossRef] [PubMed]

34. Muller, P.A.J.; Vousden, K.H. Mutant p53 in cancer: New functions and therapeutic opportunities. *Cancer Cell* **2014**, *25*, 304–317. [CrossRef]

35. Bae, Y.H.; Shin, J.M.; Park, H.J.; Jang, H.O.; Bae, M.K.; Bae, S.K. Gain-of-function mutant p53-R280K mediates survival of breast cancer cells. *Genes Genom.* **2014**, *36*, 171–178. [CrossRef]

36. Fu, Y.; Zou, T.; Shen, X.; Nelson, P.J.; Li, J.; Wu, C.; Yang, J.; Zheng, Y.; Bruns, C.; Zhao, Y.; et al. Lipid metabolism in cancer progression and therapeutic strategies. *MedComm* **2021**, *2*, 27–59. [CrossRef]

37. Broadfield, L.A.; Pane, A.A.; Talebi, A.; Swinnen, J.V.; Fendt, S.M. Lipid metabolism in cancer: New perspectives and emerging mechanisms. *Dev. Cell* **2021**, *56*, 1363–1393. [CrossRef]

38. Bauerschlag, D.O.; Maass, N.; Leonhardt, P.; Verburg, F.A.; Pecks, U.; Zeppernick, F.; Morgenroth, A.; Mottaghy, F.M.; Tolba, R.; Meinhold-Heerlein, I.; et al. Fatty acid synthase overexpression: Target for therapy and reversal of chemoresistance in ovarian cancer. *J. Transl. Med.* **2015**, *13*, 146. [CrossRef]

39. Röhrig, F.; Schulze, A. The multifaceted roles of fatty acid synthesis in cancer. *Nat. Rev. Cancer* **2016**, *16*, 732–749. [CrossRef]

40. Kumarakulasingham, M.; Rooney, P.H.; Dundas, S.R.; Telfer, C.; Melvin, W.T.; Curran, S.; Murray, G.I. Cytochrome p450 profile of colorectal cancer: Identification of markers of prognosis. *Clin. Cancer Res.* **2005**, *11*, 3758–3765. [CrossRef]

41. Keber, R.; Motaln, H.; Wagner, K.D.; Debeljak, N.; Rassoulzadegan, M.; Ačimovič, J.; Rozman, D.; Horvat, S. Mouse knockout of the cholesterogenic cytochrome p450 lanosterol 14α-demethylase (Cyp51) resembles antley-bixler syndrome. *J. Biol. Chem.* **2011**, *286*, 29086–29097. [CrossRef] [PubMed]

42. Martínez-Botas, J.; Ferruelo, A.J.; Suárez, Y.; Gómez-Coronado, D.; Lasunción, M.A. Induction of apoptosis in p53-null HL-60 cells by inhibition of lanosterol 14-α demethylase. *Biochimie* **1998**, *80*, 887–894. [CrossRef] [PubMed]

43. Mayengbam, S.S.; Singh, A.; Pillai, A.D.; Bhat, M.K. Influence of cholesterol on cancer progression and therapy. *Transl. Oncol.* **2021**, *14*, 101043. [CrossRef] [PubMed]

44. Centonze, G.; Natalini, D.; Piccolantonio, A.; Salemme, V.; Morellato, A.; Arina, P.; Riganti, C.; Defilippi, P. Cholesterol and Its Derivatives: Multifaceted Players in Breast Cancer Progression. *Front. Oncol.* **2022**, *12*, 906670. [CrossRef]

45. Niendorf, A.; Nägele, H.; Gerding, D.; Meyer-Pannwitt, U.; Gebhardt, A. Increased LDL receptor mRNA expression in colon cancer is correlated with a rise in plasma cholesterol levels after curative surgery. *Int. J. Cancer* **1995**, *61*, 461–464. [CrossRef]

46. Wang, C.; Li, P.; Xuan, J.; Zhu, C.; Liu, J.; Shan, L.; Du, Q.; Ren, Y.; Ye, J. Cholesterol Enhances Colorectal Cancer Progression via ROS Elevation and MAPK Signaling Pathway Activation. *Cell. Physiol. Biochem.* **2017**, *42*, 729–742. [CrossRef]

47. Guillaumond, F.; Bidaut, G.; Ouaissi, M.; Servais, S.; Gouirand, V.; Olivares, O.; Lac, S.; Borge, L.; Roques, J.; Gayet, O.; et al. Cholesterol uptake disruption, in association with chemotherapy, is a promising combined metabolic therapy for pancreatic adenocarcinoma. *Proc. Natl. Acad. Sci. USA* **2015**, *112*, 2473–2478. [CrossRef]

48. Gallagher, E.J.; Zelenko, Z.; Neel, B.A.; Antoniou, I.M.; Rajan, L.; Kase, N.; LeRoith, D. Elevated tumor LDLR expression accelerates LDL cholesterol-mediated breast cancer growth in mouse models of hyperlipidemia. *Oncogene* **2017**, *36*, 6462–6471. [CrossRef]

49. Menendez, J.A.; Lupu, R. Fatty acid synthase and the lipogenic phenotype in cancer pathogenesis. *Nat. Rev. Cancer* **2007**, *7*, 763–777. [CrossRef]

50. Sebastiano, M.R.; Konstantinidou, G. Targeting long chain acyl-coa synthetases for cancer therapy. *Int. J. Mol. Sci.* **2019**, *20*, 3624. [CrossRef]

51. Cui, Y.; Xing, P.; Wang, Y.; Liu, M.; Qiu, L.; Ying, G.; Li, B. NADPH accumulation is responsible for apoptosis in breast cancer cells induced by fatty acid synthase inhibition. *Oncotarget* **2017**, *8*, 32576–32585. [CrossRef] [PubMed]

52. Alwarawrah, Y.; Hughes, P.; Loiselle, D.; Carlson, D.A.; Darr, D.B.; Jordan, J.L.; Xiong, J.; Hunter, L.M.; Dubois, L.G.; Thompson, J.W.; et al. Fasnall, a Selective FASN Inhibitor, Shows Potent Anti-tumor Activity in the MMTV-Neu Model of HER2+ Breast Cancer. *Cell Chem. Biol.* **2016**, *23*, 678–688. [CrossRef] [PubMed]

53. Liang, Y.C.; Wu, C.H.; Chu, J.S.; Wang, C.K.; Hung, L.F.; Wang, Y.J.; Ho, Y.S.; Chang, J.G.; Lin, S.Y. Involvement of fatty acid-CoA ligase 4 in hepatocellular carcinoma growth: Roles of cyclic AMP and p38 mitogen-activated protein kinase. *World J. Gastroenterol.* **2005**, *11*, 2557. [CrossRef] [PubMed]

54. Sánchez-Martínez, R.; Cruz-Gil, S.; de Cedrón, M.G.; Álvarez-Fernández, M.; Vargas, T.; Molina, S.; García, B.; Herranz, J.; Moreno-Rubio, J.; Reglero, G.; et al. A link between lipid metabolism and epithelial-mesenchymal transition provides a target for colon cancer therapy. *Oncotarget* **2015**, *6*, 38719. [CrossRef]

55. Orlando, U.D.; Castillo, A.F.; Medrano, M.A.R; Solano, A.R.; Maloberti, P.M.; Podesta, E.J. Acyl-CoA synthetase-4 is implicated in drug resistance in breast cancer cell lines involving the regulation of energy-dependent transporter expression. *Biochem. Pharmacol.* **2019**, *159*, 52–63. [CrossRef]

56. Warburg, O. On the origin of cancer cells. *Science* **1956**, *123*, 309–314. [CrossRef]

57. Vasan, K.; Werner, M.; Chandel, N.S. Mitochondrial Metabolism as a Target for Cancer Therapy. *Cell Metab.* **2020**, *32*, 341–352. [CrossRef]

58. Lim, S.O.; Li, C.W.; Xia, W.; Lee, H.H.; Chang, S.S.; Shen, J.; Hsu, J.L.; Raftery, D.; Djukovic, D.; Gu, H.; et al. EGFR Signaling Enhances Aerobic Glycolysis in Triple-Negative Breast Cancer Cells to Promote Tumor Growth and Immune Escape. *Cancer Res.* **2016**, *76*, 1284–1296. [CrossRef]

59. Lampa, M.; Arlt, H.; He, T.; Ospina, B.; Reeves, J.; Zhang, B.; Murtie, J.; Deng, G.; Barberis, C.; Hoffmann, D.; et al. Glutaminase is essential for the growth of triple-negative breast cancer cells with a deregulated glutamine metabolism pathway and its suppression synergizes with mTOR inhibition. *PLoS ONE* **2017**, *12*, e0185092. [CrossRef]

60. Wright, H.J.; Hou, J.; Xu, B.; Cortez, M.; Potma, E.O.; Tromberg, B.J.; Razorenova, O.V. CDCP1 drives triple-negative breast cancer metastasis through reduction of lipid-droplet abundance and stimulation of fatty acid oxidation. *Proc. Natl. Acad. Sci. USA* **2017**, *114*, E6556–E6565. [CrossRef]

61. Tsvetkov, P.; Coy, S.; Petrova, B.; Dreishpoon, M.; Verma, A.; Abdusamad, M.; Rossen, J.; Joesch-Cohen, L.; Humeidi, R.; Spangler, R.D.; et al. Copper induces cell death by targeting lipoylated TCA cycle proteins. *Science* **2022**, *375*, 1254–1261. [CrossRef] [PubMed]

62. Zhou, J.; Yu, Q.; Song, J.; Li, S.; Li, X.-L.; Kang, B.; Chen, H.-Y.; Xu, J.-J. Photothermally Triggered Copper Payload Release for Cuproptosis-Promoted Cancer Synergistic Therapy. *Angew. Chem. Int. Ed.* **2022**, *62*, e202213922. [CrossRef] [PubMed]

63. Lei, M. The MCM Complex: Its Role in DNA Replication and Implications for Cancer Therapy. *Curr. Cancer Drug Targets* **2005**, *5*, 365–380. [CrossRef] [PubMed]

64. Zeng, T.; Guan, Y.; Li, Y.K.; Wu, Q.; Tang, X.J.; Zeng, X.; Ling, H.; Zou, J. The DNA replication regulator MCM6: An emerging cancer biomarker and target. *Clin. Chim. Acta* **2021**, *517*, 92–98. [CrossRef] [PubMed]

65. Williams, A.K.; Dasilva, S.C.; Bhatta, A.; Rawal, B.; Liu, M.; Korobkova, E.A. Determination of the drug-DNA binding modes using fluorescence-based assays. *Anal. Biochem.* **2012**, *422*, 66–73. [CrossRef]

66. Liu, L.; Mo, J.Y.; Rodriguez-Belmonte, E.M.; Lee, M.Y.W.T. Identification of a fourth subunit of mammalian DNA polymerase delta. *J. Biol. Chem.* **2000**, *275*, 18739–18744. [CrossRef]

67. Kashkin, K.; Chernov, I.; Stukacheva, E.; Monastyrskaya, G.; Uspenskaya, N.; Kopantzev, E.; Sverdlov, E. Cancer specificity of promoters of the genes controlling cell proliferation. *J. Cell. Biochem.* **2015**, *116*, 299–309. [CrossRef]

68. Zhang, L.; Yang, W.; Zhu, X.; Wei, C. p53 inhibits the expression of p125 and the methylation of POLD1 gene promoter by downregulating the Sp1-induced DNMT1 activities in breast cancer. *OncoTargets Ther.* **2016**, *9*, 1351–1360. [CrossRef]

69. Qin, Q.; Tan, Q.; Li, J.; Yang, W.; Lian, B.; Mo, Q.; Wei, C. Elevated expression of POLD1 is associated with poor prognosis in breast cancer. *Oncol. Lett.* **2018**, *16*, 5591–5598. [CrossRef]

70. Liang, Z.J.; Wan, Y.; Zhu, D.D.; Wang, M.X.; Jiang, H.M.; Huang, D.L.; Luo, L.F.; Chen, M.J.; Yang, W.P.; Li, H.M.; et al. Resveratrol Mediates the Apoptosis of Triple Negative Breast Cancer Cells by Reducing POLD1 Expression. *Front. Oncol.* **2021**, *11*, 569295. [CrossRef]

71. Kumar, H.; Kumar, R.M.; Bhattacharjee, D.; Somanna, P.; Jain, V. Role of Nrf2 Signaling Cascade in Breast Cancer: Strategies and Treatment. *Front. Pharmacol.* **2022**, *13*, 1357. [CrossRef]

72. Corazzari, M.; Gagliardi, M.; Fimia, G.M.; Piacentini, M. Endoplasmic reticulum stress, unfolded protein response, and cancer cell fate. *Front. Oncol.* **2017**, *7*, 78. [CrossRef]

73. Asadzadeh, Z.; Safarzadeh, E.; Safaei, S.; Baradaran, A.; Mohammadi, A.; Hajiasgharzadeh, K.; Derakhshani, A.; Argentiero, A.; Silvestris, N.; Baradaran, B. Current approaches for combination therapy of cancer: The role of immunogenic cell death. *Cancers* **2020**, *12*, 1047. [CrossRef]

74. Krysko, D.V.; Garg, A.D.; Kaczmarek, A.; Krysko, O.; Agostinis, P.; Vandenabeele, P. Immunogenic cell death and DAMPs in cancer therapy. *Nat. Rev. Cancer* **2012**, *12*, 860–875. [CrossRef]

75. Kaur, P.; Johnson, A.; Northcote-Smith, J.; Lu, C.; Suntharalingam, K. Immunogenic Cell Death of Breast Cancer Stem Cells Induced by an Endoplasmic Reticulum-Targeting Copper (II) Complex. *ChemBioChem* **2020**, *21*, 3618–3624. [CrossRef]

76. Schmitt, F.C.; Longatto Filho, A.; Lopes, J.M. Angiogenesis and Breast Cancer. *J. Oncol.* **2010**, *2010*, 576384. [CrossRef]

77. Ayoub, N.M.; Jaradat, S.K.; Al-Shami, K.M.; Alkhalifa, A.E. Targeting Angiogenesis in Breast Cancer: Current Evidence and Future Perspectives of Novel Anti-Angiogenic Approaches. *Front. Pharmacol.* **2022**, *13*, 485. [CrossRef]

78. Shao, J.; Liu, X.; Zhu, L.; Yen, Y. Targeting ribonucleotide reductase for cancer therapy. *Expert Opin. Ther. Targets* **2013**, *17*, 1423–1437. [CrossRef]

79. Zhuang, S.; Li, L.; Zang, Y.; Li, G.; Wang, F. RRM2 elicits the metastatic potential of breast cancer cells by regulating cell invasion, migration and VEGF expression via the PI3K/AKT signaling. *Oncol. Lett.* **2020**, *19*, 3349–3355. [CrossRef]